6TH INTERNATIONAL CONFERENCE ON DAM ENGINEERING
C.Pina, E.Portela, J.Gomes (ed.)
Lisbon, Portugal, February 15-17, 2011

MODELING THE START OF THE EXPANSION DUE TO ALKALI SILICA REACTION IN CONCRETE

Luís Mayor Gonzalez[*], António Santos Silva[†], Dora Soares[‡], Said Jalali[*]

[*]Departamento de Engenharia Civil, Universidade do Minho,
Campus de Azurém, 4800-058 Guimarães, Portugal
e-mail: lmgonzalez@mail.telepac.pt

Keywords: AAR, Reaction start, prevision, service life

Abstract. *Service life of a concrete affected by alkali-silica reactions (ASR) is the age at which expansion is no longer allowed for normal use of a structure; such expansion level depends on the application. Once the induction period ends, the expansion proceeds quickly.*

Thus, in the present study, the service life was approached by the induction time.
Induction time is an abstract concept, its formulation depending on the model considered (additive, constant time in the diffusion model, or the abscissa of intersection of time axis by a tangent to the expansion curve at the inflexion point, in the nucleation and growth model).

Mortar bars were made with Tagus river reactive aggregate according the ASTM C 1260 procedure (expansion of bars immersed in NaOH 1M) implemented at temperatures of 80, 70, 60, 50 and 37ºC, to model expansion at constant alkalinity, considering the aggregate reactivity and temperature as variables. The results show that the data has enough precision for a kinetic study.

Two kinetic models were considered to fit the data, selecting one of which for further improvement, using the wide information basis on the ASR.

The effects of the factors temperature, alkalinity and humidity assumed models referred to in literature, or obtained by regression both of kinetic parameters for each isothermal curve and their temperature coefficients of Arrhenius plots. The correlations obtained allow estimating the strain after the induction period, for any value of the mentioned factors, under laboratory conditions.

The model estimates at ca 37ºC were compared with experimental data in the same setup and this temperature. The induction time prediction was satisfactory, but further expansion development pattern was different.

The model was tentatively applied to a case reported in letterature. Results match, but are affected by significant errors, some improvements being referred to improve accuracy.

[†] Laboratório Nacional de Engenharia Civil (LNEC), Av. do Brasil, 101, 1700-066 Lisboa, Portugal
e-mail: ssilva@lnec.pt, webpage: http://www.lnec.pt
[‡] Laboratório Nacional de Engenharia Civil (LNEC), Av. do Brasil, 101, 1700-066 Lisboa, Portugal

1 INTRODUCTION

The alkali-silica reaction (ASR) in concrete is a deleterious pathology that limits the durability of concrete constructions. It occurs as a system of physical and chemical transformations within concrete, when and where all conditions required are met: reactive aggregate, enough alkalis in the concrete pore solution from the concrete starting materials (cement, aggregate or water), micro-environment or anthropogenic source, and humidity. Temperature also affects the rate of the reaction. Some supplementary cementitious materials (SCM's), like fly ash, metakaolin, pozzolans, or simply finely ground reactive aggregate, if added initially to the concrete mix in the proper amounts, can act as suppressors.

Swamy 92 [1] pointed out the internal nature of the processes: once started it can just be delayed, e.g. by humidity isolation, but will go on as this restraint is removed, at faster pace, as Larive 98 [2] showed experimentally, until the expansion equals the same it would have reached without that restraint. As a result, any factor affecting the reaction rate affects as well the service life.

At the project stage it is possible to choose appropriate combinations of aggregate, cement, water and SCM's to fit the requirements for service life. But it may have a cost to find the suitable combination of materials so that some trade off must be made, and that is possible only with new construction. Broekmans 2010 [3] indicate an expenditure of 2 GEuros annually in maintenance and reconstruction of structures affected by ASR.

Due to the economic importance of concrete buildings and infrastructure, models to predict expansions due to ASR have been developed, particularly for large infrastructures such as dams. These account not only for the reaction itself but for several of its effects on the expansion of the modeled structures, and stress accumulation generated by expansion on other parts of the structures themselves. To foresee the first problems to occur, usually considered to be related to structures deformation and misalignment of moving parts such as gates and generators, expansion modeling range may require to include deformations as low as 0.02% for dams [4] , even lower than the level of 0.04%, generally considered for early cracking to occur.

The present paper adopted a different approach, for situations less size-sensitive to expansion. In general, the reaction is known to progress slowly, sometimes for decades, before being detected, and after the first micro-cracking starts, its rate increases. This is explained by some authors, e.g. Larive 1998 [2], as due to a diffusion controlled process, where microstructure variations due to cracking of aggregate particles and the cement paste improve diffusion conditions (the term used, "change of diffusional regime", is appropriate). Also, it seems logical that, in aggregates surrounded by a porous paste imbibed in alkaline pore solution, this is pumped into the cracks as they open, by the suction due to the outwards expansion of the periphery from the core, so that contact between reagents may be promoted.

In other words, reagents and products diffusion is initially restrained by the low permeability of the cement paste and the aggregate (as described by Poyet 2003 [5] for the Furusawa model).

The underlying processes are not consensual, different mechanisms being claimed [5, 6]. Poyet 2003 [5], for instance, describes four reaction mechanisms (imbibing and swelling, nonequilibrium thermodynamics, electrical layers repulsion, structural disorder), with different expansion mechanisms. Wigum 1995, 2006 [7, 8] refers two aspects being present. As they are the most referenced, they are briefly described.

The classic explanation is that the reaction takes place by steps, opening the siloxane bridges of the silica structure and neutralizing the silanol groups formed that way, until silica dissolves into pore solution, from which it precipitates as a gel, in the presence of calcium, possibly enclosing entire portions of the solution. The gel produced is hygroscopic, and expands on absorbing water, generating expanding pressures enough to crack the aggregate and the paste. The cracking of aggregate then allows the reaction to continue. Several mechanisms are also pointed to explain the formation of gel and its expansive properties.

For the other mechanism, most of the expansion occurs inside the aggregate. The same steps generate a local change which expands the crystalline structure, forming an amorphized solid, sometimes described as a first, or dry, gel, that may further expand locally by adsorbing alkali ions and water. As a result of the reaction, preferentially on the aggregate periphery, the particle expands in a non uniform way, generating a field of stresses within it [9, 10]) that led to tangential and radial cracking, some of the cracks extending radially into the cement paste (as described by Pade and Struble [11]), so that diffusion and the related processes are accelerated. Wigum 95 [8] considers this last aspect to be the responsible for the expansion and cracking observed.

Whichever mechanisms are operating, measurable global outputs, beyond expansion and change of mechanical properties, are consumption of hydroxyl ions, of four coordinated silica tetrahedra, of silanol groups (initial or formed in the process), and, more difficult to observe and measure, of local portlandite. Also, macro cracks appear external to the concrete as three-armed map cracking, and micro cracks can be observed inside the aggregates and the paste, resulting in an increase in porosity.

Gel also appears, both inside the cracks and the boundary between aggregate and paste (Rivard 2003 [12] observed it inside the aggregate; other authors refer its presence around the aggregate or in its rim), Scrivener 2009 [4] refers that the appearance of gel inside the aggregates is often seen before paste starts cracking. The gel sometimes accumulates into the paste cracks with a flow pattern resembling a glacier overview, migrating through the cracks opened by the reaction inside concrete, from which it may exude, or just be visible deep in the external cracks.

In this sense, this transition from a non cracked, lower permeability state to a cracked and higher permeability state is the critical point that defines the reaction rate marked increase and the beginning point of the deterioration process. It is, as referred to, the change of diffusional regime mentioned by Larive 98 [2].

The present approach is to describe this in chemical kinetics terms: as expansion is very slow and suddenly accelerates, the first period may be considered as an induction time of the overall process. The current methods used in chemical kinetics to predict induction time might then be used to predict the period before deterioration starts.

Induction time however is an abstract term. Its particular formulation must be adapted to each model considered in a slight different way. These are discussed below for several reaction kinetics models usually referred to in the literature.

Although reactivity tests are designed to characterize the aggregate, they measure essentially kinetic phenomena, and its relative simplicity and wide use and resulting accumulated information were considered as a good basis to develop, based on their setup, a method for determining the induction time.

It is interesting to note that reactivity, a kinetics related aggregate property measured in so many different ways, has been used to formulate implicitly the effects on service life, even without direct kinetic observations, e.g., by the rejection or limitations on use of aggregates containing reactive components just from geological or petrographic examination. Moranville Regourd [13] cites Bochiorrini as indicating a close relation between time of appearance of cracks in concrete and the disorder coefficient of silica in the aggregate, determined by Infra-Red spectroscopy to determine reactivity. Probably a similar relation might be developed for Quartz Cristallinity Index, a parameter measured by XRD, which Katayama [14] has shown to be correlated to the dissolved silica in ASTM C 289 test [15] for some Japanese aggregates. Also Furusawa et al 94 [16] developed a model to predict ASR derived expansion from data taken from a modification of ASTM C 289 [15] reactivity test. More recently Shon 2008 [17] used dilatometer tests to evaluate the apparent energy of activation of the reaction, to establish the time scale factor allowing to predict expansions at different temperatures using a performance based approach.

Among the available reactivity tests, the ASTM C 1260 [18] test seems well suited for this purpose. In it, the alkali concentration is nearly constant as reaction proceeds due to the large volume of alkaline solution, differently from a common concrete application where the solution it simulates is confined to the concrete pores. In fact the alkali contents, once established in concrete, is only nearly constant just in the beginning, when induction is developing, reaction rates and its reagents consumption are low.

This allows, in the expansion measurements by this method, to isolate the changing alkalinity factor from expansion, so that it is possible to project back to the beginning the fitted curve obtained from expansions above the critical transition.

To allow using data taken from tests on an aggregate in different applications, it is necessary to consider the effect of changing concrete conditions such as alkali content and humidity. The main factors of ASR were used for this, assuming existing models of their effects, taken from separate studies in the literature or other relevant models. These assumptions are discussed below.

The proposed method was developed using as study case, data from tests using a reactivity test setup, on Tagus river reactive aggregate at different temperatures.

2 RELEVANT FEATURES OF THE REACTION, ASSUMPTIONS AND MODELS CONSIDERED

2.1 Morphology of the reaction progress

Different morphologies are described for the affected particles. This may not necessarily imply deep differences in the process, being a complex reaction, as variations of the relative rate of the partial transformation may render some aspect dominant.

Cracking, micro or macro, is one of the visible features of the ASR. At micro level, descriptions have been made sometimes with conflicting aspects.

Figures 1-4 display two such morphologies, with two common situations, of mono and polycrystalline particles of quartz, in each case an image (right) of an impregnated sample with fluorescent dye to highlight the porosity by means of resin penetration, and (left) in nearly crossed polars evidencing the polycrystalline formation and the inter or intracrystallite resin penetration.

The first field (figures 1 and 2) shows 3 polycrystalline grains with varying intercrystallite attack (evidenced by resin penetration), and a mono crystalline grain. In all grains an unreacted core is present, with differing depths of attack, somewhat progressive.

The second field (figures 3 and 4) displays typical undulatory monocrystalline quartz, with tangential and radial cracks, concentrated in the regions of higher curvature.

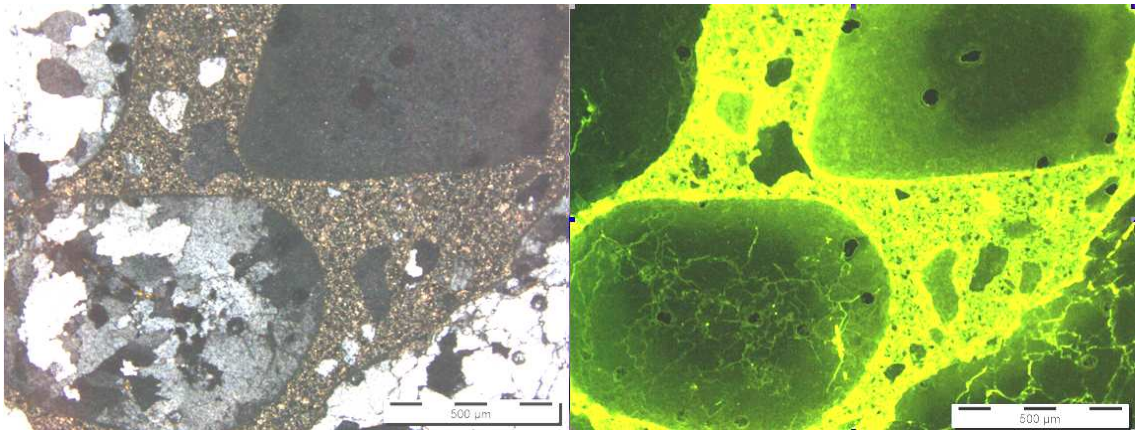

Figures 1 and 2: Several polycrystalline grains and, upper right, a monocrystalline one. Resin penetrates both in poly and mono crystalline grains, apparently with two factors: the inter-crystallites cracks and the distance to the periphery. Unaffected cores are better evidenced at grain level rather than at crystallite level. In the monocrystalline grain the penetration displays a diffuse front, forming blocks progressively smaller outside, i.e. higher reaction time, in an unsymmetrical way. *in Gonzalez 2010 [19]*

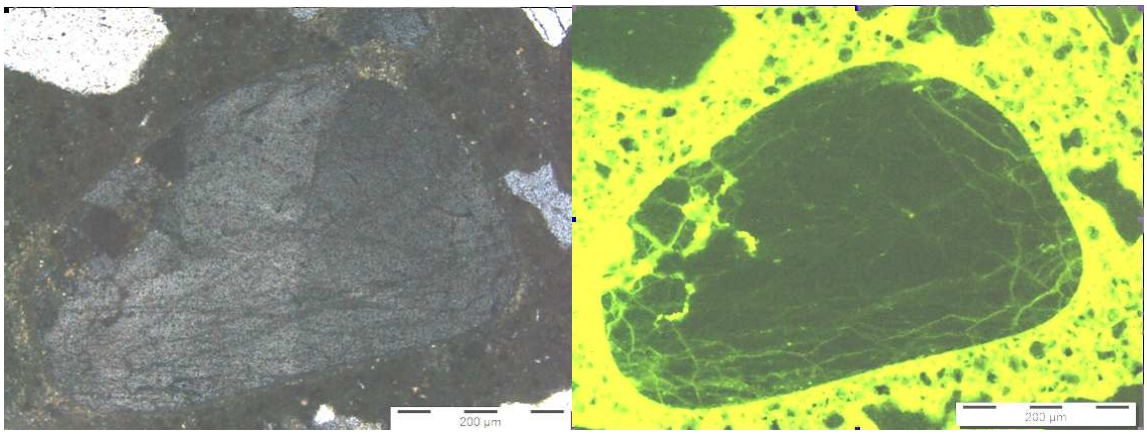

Figures 3 and 4: A monocrystalline grain shows deformation at nearly crossed polars and, by resin penetration, intracrystallite microcracking, peripheral. A general cracking pattern, formed by tangential and radial cracks, is denser near higher curvature regions and leaves a less affected core. The pattern suggests preferential and peripheral expansion (cf Golterman 94,95 [9, 10], Pade and Struble 2000 [11]). *in Gonzalez 2010 [19]*

The figures suggest that the reaction, being more developed at the periphery, proceeds inwards. The radial fissure, lower left corner of grain in figure 4, disappears midway to center. It is assumed that the reaction locally produce an expansion (by lattice modification or gel swelling) leading to local cracking, through which diffusion of hydroxyls, alkaline and silicate ions, water and gel itself can take place at faster pace. Consequently, an unaffected core is gradually shrinking due to the reaction progress. It is assumed that at least in the early reaction, its extent can be described by the volume of the cracked, expanding zone, as described below.

2.2 Modeling of the main factors affecting the reaction

The main factors for the reaction are indicated below. It is necessary to account for their possible variation and effect on the reaction extent and expansion.

Reactivity. The reaction affects expansion, but is also monitored by it. This relation is sometimes understood as a duality, the expansion being taken by many authors as the reaction progress itself (e.g. Larive 98 [2], in the development of her model). Ben Haha 2006 [20] has studied the relationship between both, for certain aggregates [4].

Expansion is also the most significant effect for modeling, as it may easily be associated or translated into stresses and combined with other factors to predict the development. So using expansion as the measured reaction parameter has the advantage of cancelling possible errors due to conversion between expansion and reaction extent.

In this paper, a relation between both is tentatively presented, based only on geometrical considerations and the concrete constitution, assuming that reaction taking place locally induce a local expansion of the aggregate, that is converted into concrete expansion by the aggregate skeleton. Cracking, and the volume increase it induces, is considered as a constant, proportional, side effect.

Alkalinity. The reaction is assumed as first order on the contents of hydroxyl ions in pore solution. To relate this concentration to the alkali contents of the cement, generally considered as its main source, the Helmut 93 [21] empirical correlation is used.

$$[OH^-]\text{, mol/L} = 0.339\ Na_2O_{eq}\ \% / (a/c) + 0.022 \pm 0.06 \qquad (1)$$

where w/c = water / cement ratio. This equation yields the "initial" alkalinity in hardened concrete, after hydration. The ASR itself as well as leaching by water or high relative humidity environment lowers the alkalinity thus estimated. When using long tests with immersed bars, the alkalinity of the surrounding environment is assumed. This seems logical and supported by experimental observation (ASTM C 1260 [18] states that the alkali content of the cement has no significant effect on expansion).

Humidity. Humidity is a factor affecting expansion in multiple ways: directly through the aggregate, gel and the cement paste sensitivity, but also by conditioning mass transfer between environment and pore solution, and affecting alkalinity through drying, condensing and leaching. A global relation was taken from the modeling of Capra et al [22] of the Poole [1] graphical formulation of its effect.

$$\text{Humidity correction factor} = (HR/100)^8 \qquad (2)$$

Temperature. The reaction is thermo activated, and there is a consensus that the rate of reaction follows an Arrhenius law

$$\ln(1/K) = k1 \cdot \exp(-Ea/RT) \qquad (3)$$

where ***K*** is the kinetic constant of the reaction, **k1** is the pre-exponential constant, ***Ea*** the apparent energy of activation, ***R*** the ideal gases constant and ***T*** the absolute temperature, in Kelvin degrees.

2.3 Models considered and selected

Models of the ASR development usually are concerned with its effects on a particular structure, and depend not only on the internal expansion, but on particular dimensions, reinforcement orientation, environmental conditions and interexchange, outside stresses, and constraints. These are usually applied to an elementary representative volume, connected to the surrounding ones by displacements and stresses. Overall structure evolution is then simulated by numerical integration by finite elements.

In the present approach for induction time modeling, only the kinetics of the reaction or the expansion directly related is relevant and can be addressed by general kinetic models or models developed specifically for this reaction, such as the Larive model.

Several classical articles (Diamond et al 1981 [23], Glasser 1992 [1], Poole 1992 [1], Larive 98 [2]) defend diffusion as a relevant, if not controlling, step. It must be said that the energy requiring breaking of siloxane bridges is also presented as controlling, i.a., by Bulteel et al 1999 [24].

General kinetic models for solid-fluid reactions allow considering induction time, either by a constant added to the "internal reaction" time, as a time lag, or as a specific parameter in some models. A general discussion on the use of several models for time induction evaluation was carried out by Gonzalez et al 2001 [25]. The so called reactions with sigmoidal curve of conversion cover a large number of possible variations and mechanisms such as, a few of which might be relevant:

- initial diffusion of reactants to interface,
- adsorption of the reactant to the active sites,
- microstructure changes of several types:
    - fragmenting of solid particles into smaller units,
    - opening access to reactant diffusion across the initial interface product layer blocking contact between reactants, by:
        - dissolution,
        - local fragmentation of the product layer deposited at the interface, or
        - modifying the reaction to yield a porous product
- reaction in several sequential stages or steps

To these, classical models are added, with a transient initial period of activation, or removal of a resistance, so that the curve shape means little. It is more important to find a good model fitting the rest of curve and the relation between curves, at several temperatures and concentrations, and try to establish an appropriate time lag with a crude, simpler model.

Several studies on ASR have considered the nucleation and growth model (Avrami, Erofeev or Kolmogorov), e.g., Jonhston et al. [26], Pade and Struble [11]. Shon 2008 [17] reviews many of these applications.

Models specific for this reaction were reviewed by Moranville-Regourd 97 [27] and Poyet 2003 [5]. Recently, Scrivener 2010 [28] presented a model of this type.

Although having developed an independent model, Larive 98 [2] considers in her review that diffusion is probably the controlling factor, an idea also found in Glasser 92 [1].

After studying the microstructure of the aggregate and the progress of reaction shrinking the unaffected core, the present study considered diffusion with induction time, as explained above, and nucleation and growth models as appropriate for a first data fitting.

Beyond providing a sigmoidal curve as model, the reason for nucleation and growth model has been seen by some authors [Moranville 97 [27], Furusawa et al 94 [16], Diamond 1981 [23], Ichikawa 2007 [29], Glasser 1981 [30]] as referring to an initial period in which gel is formed and occupy empty spaces within or around the aggregate particles, after which pressure rises while volume is confined.

The induction time is directly a parameter in the diffusion model with induction time, but the Avrami or Erofeev model doesn't have any such parameter or term, or consider any initial stage where conditions are different; in fact it applies uniformly, from beginning to the end of reaction. For comparison purposes, however, the time of induction may be estimated by the equations advanced by Gonzalez et al 2001 [25], using this model to find the abscissa of the

point where the time axis is crossed by a tangent to the inflexion point.

Both models fit very well in the period after cracking to isotherms data obtained as described below, but the model parameters thus obtained fit somewhat less well in the Arrhenius relationship with temperature, particularly in the case of Avrami model.

However, Jonhston et al [26] indicated, for the Avrami model, a dependence on alkalinity of the exponent **M**, itself already with a not well defined dependence on temperature.

In the present case the flexibility for this variation was supposed to be needed, and the Avrami model was discarded.

With the diffusion model with induction time, a classical model in kinetics, an initial discontinuity is forced that limits the precision in the initial period (though ASR is supposed not to be relevant at this stage, and expansion is set to zero; this is just an approximation, not what experiments show, as it will be seen below). Alkalinity was assumed as constant, given the high excess of alkalis in the immersion bath).

2.4. Assumptions for model development

The reactant in the fluid attacks the solid only at the material most reactive zones, around active sites or activated areas like displacements, pores, cracks and others, forming pores and cracks that shrink the unaffected core. Conventionally, the residual part is designated as ash and is inert – in this case, probably is not completely inert, but at least reacts slower.

The existence of an unaffected core, sharply defined, *strictu sensu*, is an auxiliary assumption. Although in some reactions visible rims do exist, the microstructure alteration as cracking begins is usually random and chaotic, and a reaction front, even diffuse, is more guessed than defined by cracks, ions concentration and micro hardness profiles, Scrivener and Monteiro [31] report for the opal/cement paste a continuous variation, without any visible or measured discontinuity.

It allows however to model changes observed and so it is used in the present paper.

Granular particles are assumed ideally as spherical

In the case of a sphere, the affected part forms thus a progressively thicker spherical shell, which volume is easy to relate with depth of attack. In some cases it is described as ***a rim***; ***in others, as a more densely cracked and porous zone*** (as in figures 2 and 4); in all cases it is ***a zone where SEM-EDS detects a decrease in Si, and a rise in K, Na or/and Ca, and O (opening of siloxane bridges and adsorption of water.*** A correlation with ***micro hardness*** variation in depth was also reported by Kawamura [32].

Front progression.

The volume fraction of the shell measures the reacted fraction of the material. Considering all material as reacted (at least the more reactive one), the extent of reaction can be related to the front progression, if all particles were uniform.

These assumptions are the same as taken by the so called topochemical models, presented by Kunii and Yagi (e.g., Levenspiel 1972).

Overall Extent of Reaction and Expansion.

The expansion is the more visible and direct cause for problems, and the easier effect to monitor. The relation between extent of reaction and expansion is however a matter of discussion. Some authors simply consider them to be equivalent or proportional.

A local expansion due to reaction is reported by several authors, referring it to increase in volume at crystal lattice level due to conversion from tetra- to tri-coordinated silicium tetrahedrons, to alkali ion adsorption and alkali gel formation, to alkali-gel expansion by water up taking, by zeta potential variation due to ionic changes in environment.

Whichever the real cause, it is assumed that the reaction produces an increase of local volume that expands the outer shell. The shell expansion is one of possible causes for early

cracking, which may promote its permeability and so, diffusion. From local to global expansion, also different mechanisms are reported, some of which consider an amplification factor for some aggregates, such as siliceous limestone.

The outer shell itself propagates the expansion to the skeleton and the structure itself. Not all the particles are reactive, and their expansion certainly distorts the structure and contributes to cause additional cracks. Any of these steps is not easy to model, and in the scope of this work, they are not considered in detail.

3 EXPERIMENTAL

Tagus river reactive aggregate was used to prepare mortar bars, according to ASTM C 1260 method [18]. Three bars for each test temperatures (80, 70, 60, 50 and 38ºC), subject to the same conditions (expansion of bars immersed in NaOH 1M).

Expansion measurements were made at 0, 3, 5, 7, 10, 14, 21, and 28 days, and weekly after that for the lower temperatures, to model expansion at that alkalinity and several temperatures. At these ages, the presence of gel exudation on the bars and in the solution was checked and, whenever observed, registered.

Each isotherm expansion curve is a plot of the average readings for three bars versus time.

In a subsequent stage the last temperature was tested for a longer period, at a nominally 38ºC temperature controlled chamber. Temperature was measured and checked for the longer test, the value 37.2 ºC being found.

All data were treated in EXCEL, and regression lines calculated. Analysis showed the readings to meet precision requirements for a kinetic study, the method recommended test errors not being relevant for kinetic study.

4 DATA PROCESSING, RESULTS AND DISCUSSION

To model the expansion, it was considered as the effect of several factors. Alkalinity was supposed constant and equal to 1M, and reaction as being first order in relation to it. Relative humidity (RH, %) was supposed as saturated in all tests, and its effect for other situations, according to Capra, is given by the correcting term (equation 2).

The modeling aimed to predict when reaction reaches a significant strain. This allows neglecting the expansion in the pre-cracking period, at very low expansion values.

The significant strain value depends however on the application; for a general approach, the value of 0.04% was taken for reference, conventionally considered the start of visible cracking. Values below 0.02% are referred to by Scrivener 2010 [28] as possibly relevant for dams, while rehabilitation works were decided and implemented at levels of 0.2%, as reported by Miyagawa 2006 [33]. In any case, once confirmed its appearance, progress of ASR can't be avoided, and measures must be studied to slow its rate or repair its damages, so that a level of 0.04% as limit of the pre-cracking, induction period, seems always a good reference, at least.

4.1 Fitting model with plane interface to isothermal data

The models are fitted, at each temperature, only to data with expansions above 0.04%, disregarding the initial points, and the model assumes expansion as zero for pre-cracking levels, as they are before induction time.

Initially a topochemical model was fitted, with diffusion control and plane interface (Levenspiel 1972 [34]), as used by, i.a., Furusawa et al 1994 [16], of linear dependence between time and the square of expansion, adding a constant, at each temperature, as induction time

$$t - tind = C\,(\Delta x)^2 \qquad (4)$$

4.2 Arrhenius plots

Linear Arrhenius plots ***with excellent correlation*** were obtained for the *reaction rate constants and the inverse of induction times, as yielded by this procedure for each of the* four curves at higher temperatures (80, 70, 60 e 50ºC) .

The regression lines representing those kinetic parameters inserted in the equation above then model the expansion in time for any temperature, in the period after cracking. The dependence on alkalinity and humidity is taken from literature and other models.

4.3 Model extrapolation to 37ºC

The initial data at 37ºC, didn't reach the significant expansion zone, and allowed only to conclude that although not significantly incompatible, it couldn't show compatibility as the low expansions reached were out of the model validity range.

As results were not negative, though, the test was repeated for a longer period to clarify this issue of compatibility between models and results. The test was carried out in LNEC, and ***a prediction of induction time not consistent with the experimental data obtained is*** yielded by the *kinetic model thus determined, when* extrapolated for 37 ºC, as shown in figure 5.

4.4 Model with spherical interface

Face to the divergence found, ***particles of spherical shape*** instead of plane were considered, and the model re-adapted.

The standard development of the topochemical model for spherical particles, can be found, e.g., in Levenspiel 1972 [34], or Sohn 2003 [17], based on the development of a spherical shell through which the reactant must diffuse in a fluid to reach the surface of a shrinking, spherical core (known as Unreacted Shrinking Core or UCS model**)**

$$t - tind = \rho_B R^2/(6bD_eC_A)\ \ (\Delta r/R)^2\ [1- 3(r/R)^2+2(r/R)^3)] \qquad (5)$$

where ρ_B is the density of solid reactant, **R** is the initial radius of the particle and **r** the value at time **t**, **b** is the stoichiometric ratio between reactant moles of solid and fluid, D_e is the effective diffusivity (equal to diffusivity in open space, multiplied by porosity of the spherical shell divided by tortuosity), and C_A is the concentration of reactant in fluid. Note that ρ_B refers to reactions actually taking place, which in our case, may concern only an activated part of the total silica.

As we are measuring the reaction through expansion, assuming both are proportional, it was convenient to adapt slightly the standard model, evidencing a term possible to relate more easily to the expansion itself, by simple mathematical handling, achieving:

$$t - tind = \rho_B R^2/(2bD_eC_A)\ \ (\Delta r/R)^2\ [1-(2/3)(\Delta r/R)] \qquad (6)$$

The value of **R** may be eliminated between the two members of the equation, except for the last parenthesis; if **R** grows, the equation tends to the same as in the plane interface. The model was formulated for non porous solid surrounded by fluid; the present case, assuming the cement paste with a much higher porosity than the aggregate's, is close too such situation.

The depth of attack, or progression of the reaction front, $\Delta r = R - r$, is related by

$$\Delta r /R = [1-(1- X)^{1/3}] \qquad (7)$$

with **X**, fractional extent, progress or conversion of the reaction; it is the fraction of solid reactant that was converted (it can also be defined in relation to liquid reactant if this is limiting and not changed by further additions). It is assumed that in the reaction, at least in the

beginning, which is of our concern, only material from active sites and their neighbor-hood react, this process defining the affected zone (for a rim morphology, formed by non affected material; for other morphologies the relation may be less direct).

Being **k** a constant of proportionality between bar expansion of the bar and depth of attack in reactive particles, **Δr** or **Δx**, it is **k.ε= Δr/R**, with the strain globalizing the effect of transmission from reactive particle to bar, and the effect of volume increase at each reactive particle level due too reaction progress, and all the associated transformations (chemical, microstructure and physical), the final equations are obtained as

in plane particles, $\mathbf{t = tind + C\,(\Delta x)^2 = tind + C\,(k.\varepsilon)^2,}$ (8)

in spherical particles $\mathbf{t = tind + C'\,(\Delta r/R)^2\,(1\text{-}2/3\,\Delta r/R) = tind + C'\,(k.\varepsilon)^2\,(1\text{-}2/3\,k.\varepsilon)}$ (9)

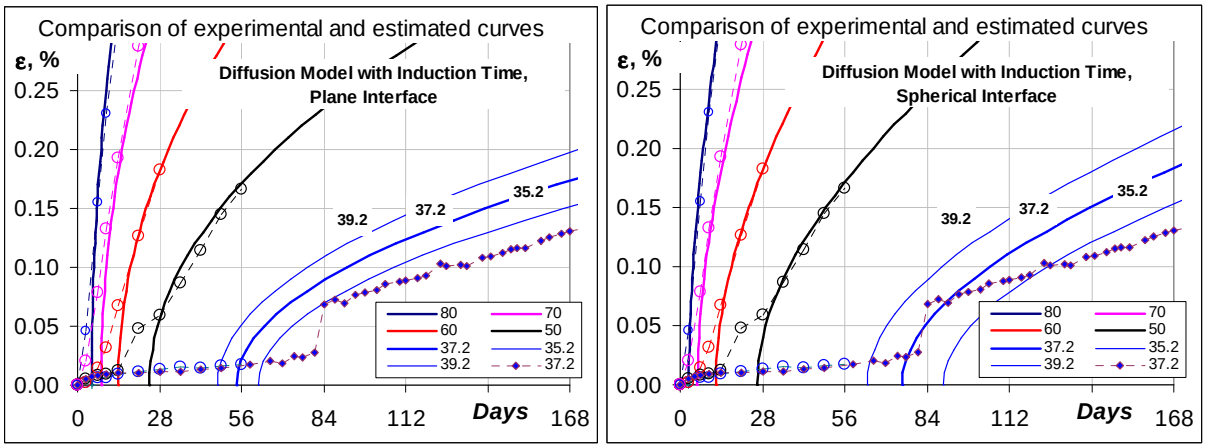

Figures 5 and 6: Comparison between experimental values and estimated by data fitting using model with plane symmetry (left) and spherical (right). The values of the curve at ca 37 ºC, initial test (circles), are not compatible in the left figure. Full diamond marks refer to repeated test, at temperature measured, more accurately, as 37.2 ºC.

As referred to, the constants **C**, **C'** e **tind**, different for each isotherm, are estimated by fitting by least squares to each isotherm. The values obtained for the kinetic parameters are then correlated with the inverse of the absolute temperature in Arrhenius plots.

The parameter **k** is fitted later directly to the data points for all temperatures simultaneously. In this example, the value obtained was **k=136**. This globalizes several effects such as the local primary expansion, the active sites concentration in the spherical shell, the concentration of reactive particles, the transmission from local to shell expansion, and the from shell to bar expansion.

The proportionality relations, constants, **C** or **C'**, with the exception of last parenthesis for the spherical particle model, are integrated in the experimental data fitting. Figures 5 and 6 allow to visualize the effect of this modification, showing the initial test at *ca* 37ºC and its repetition, at 37.2ºC, as referred to in v) and vi).

The ***results improved in a significant way*** regarding the modeling of induction time, the main target, yielding better correlation coefficients and error margins. The error margin is always large, as the statistical error is characterized by deviations of a logarithm of an exponential function, and when reverting to the exponential function, from an additive term becomes a factor after antilogarithms are applied. The number of points considered to model the equations, and its choice, may also affect these results.

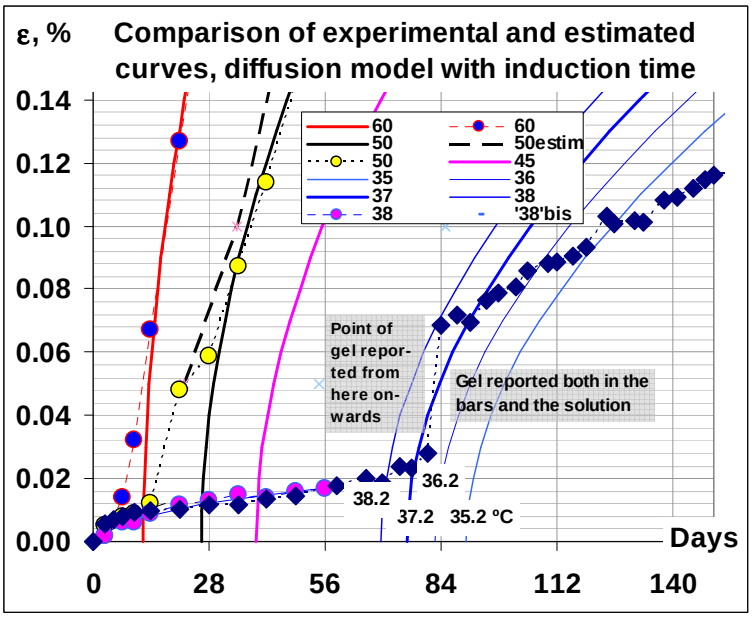

Figure 7: Comparison of experimental strain with the one given by the proposed model, detailing better the pre-cracking period.

4.5 Induction or pre-cracking period

In the pre-cracking period, expansion started immediately, very slowly, as in previous tests, and ***reached a significant level, with slight deviation, at the time foreseen to the induction time*** at that temperature (figures 5 and 6), ***when it has shown a sudden variation.*** The test temperature, nominally at 37ºC, was measured with higher accuracy as 37.2ºC; in figure 7 the curve estimated by the model at this temperature is represented, side by side with curves with this temperature plus increments of +/-1 e -2ºC. The figure also depicts isotherm data and curves at 50, 60 and 70ºC. It is easily to notice the strong influence of the temperature, which justifies the need of higher accuracy in the reading of the temperature.

The curves, averaging three measurements, suggest in figure 7 a precision higher than the real one, affected by several factors, subjective and objective.

Notice in figure 7 a drift at 37ºC from the position of the age at 0.04%, usual indicator of the visible cracking and which, in other curves, is slightly below induction time.

The expansion at 37ºC deserves an attentive look (figure 7), In the pre-cracking period there is an initial regime, until 0.012%, with curvature downwards, followed by an accelerated expansion between 0.012 and 0.028%, that ends with a sudden expansion (assumed to be cracking, but which was not possible to observe directly as such, maybe due to rugosity of the surface).

The expansion after cracking is linear, differently from the expansion foreseen by the present model (see figures 5, 6 and 7),

4.6 Comparison with model

The model herein proposed ignores the strain before cracking, only *aiming to foresee its start, what it does*. The interpretation and modeling of this pre cracking period might help to understand the processes and simulate the initial development of ASR in structures (e.g., for dams, according to Scrivener 2010 [28], the expansion zone before 0.02% should be modeled).

The expansion pattern in the pre cracking period fits neither the present model nor any of the described models does. Sigmoid shaped models (such as Avrami's and Larive's) don't fit

well a zone with downward curvature, which is dominant in the pre cracking period, well delineated at 50 and 38ºC. *A diffusion model without induction time might be considered* in the future, maybe modified to accommodate the effect of micro cracking induced changes on permeability and diffusion. But the method of reading expansions and possibly the corresponding reaction extents must be improved before going on into these matters.

5. APPLICATIONS

The proposed model compared positively with data at 37 ºC for induction time of occurrence of cracking. This was the initial objective. Predictions before and after that time are not valid, due to the model assumptions, however, a comparative evaluation is made.

In the period before cracking, it assumed all expansions to be null. In the period after cracking, the curve trend at the referred temperature is different, following a linear trend. Curiously, the unfitness of the present model for these situations is shared by the other models mentioned, diffusional or sigmoidal (in the pre-cracking period, sigmoidal models, upward curved in this zone don´t fit the downward curvature displayed by the experimental data; in the period after cracking, also none of them fits the linear trend).

The comparison was made only for temperature variation. The effects of alkalinity and humidity, given by equations 1 and 2, are however just assumed to be the same as in other kinetic models, and should be checked in tests, separately for each factor and altogether.

Possible applications for this model are restricted by this. Applications demanding both very low expansions, for the period pre-cracking and higher expansions well above induction time need a different approach.

Applications of the present model, are thus restricted to cases where prediction of the induction time of the reaction is important. This is to say, that the proposed model applies to induction period, regardless of dimensions and interaction with nearby structures, however it can be used for defining an interval of time for inspection purposes.

This model independently from the structural dimensions and interactions, allows to consider the behaviour of the structural material in itself and this allows to establish a general limit for service life applications. Thus the model enables to foresee the period of time for which the initial properties of the structural material are kept within acceptable limits.

In specific cases the service life is limited by very small deformations occurring during the induction period, or allows deformations far beyond the induction period, and other models should be used.

5.1 Application case of the model

The present model was applied for estimating the service life of a railway sleeper. The considered sleepers were used in a covered area, protected from rain (Santos Silva et al. 2008 [35]), that allows using meteorological data of temperature and humidity in the period before ASR was detected.

The influence of cement alkali contents on alkalinity was assumed as given by equation 1, for a cement alkali content of 0.693 % Na_2Oeq and w/c of 0.425. Humidity and temperature were assigned values of 16ºC and 77.5%, from a general meteorological data source. For error estimating, variations considered were HR [0.75-0.8], Na_2Oeq [0.56-0.825], w/c [0.35-0.5].

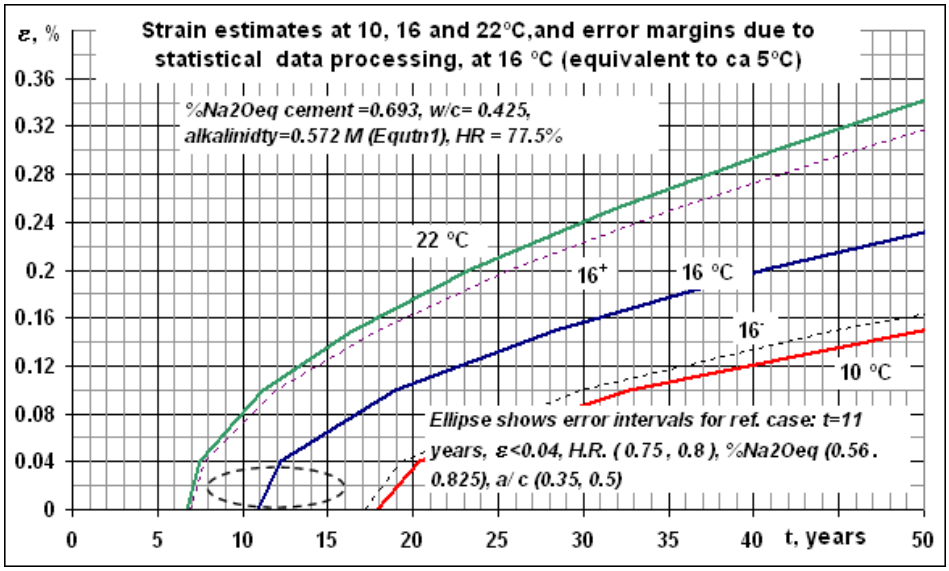

Figure 8: Deformation prediction at different temperatures (10, 16 and 22ºC); the error margins are indicated in dashed lines

Figure 8 shows that the induction period for strain under 0.04%, at 16ºC, is predicted as 11 to 12 years. This is consistent with field observations of a 11 years old sleeper, well within the error margins from statistical processing (dashed lines). Expansion curves at 10 and 22ºC are included for comparison.

In particular, it should be noted that the use of general meteorological data was useful for defining the major factors of temperature and humidity.

6 CONCLUSIONS

ASR begins immediately, but the related expansion reaches a significant level only after a slow evolution that is dealt with as an induction period. In the present model, the significant level was fixed at 0.04% in association to early cracking general consensus, and the time it takes to reach that level was defined as the induction time, which was modeled from tests carried out with the widely used ASTM C 1260 setup, at different temperatures.

A diffusion model with induction time was used, for which high correlation coefficients were met for fitting isotherm curves (at temperatures between 80 and 50ºC), extracting the two kinetic parameters (diffusional and time induction), as well as for fitting of the Arrhenius plots of these kinetic parameters.

The model was checked with data at 37ºC, for which the induction time was found in agreement with the model estimates. The model doesn´t apply for the period before cracking and was found to have a trend after cracking different from the experimental. In both these zones, however, the performance of other projects, diffusional or sigmoidal, are not expected to be good. Posssible improvements for both areas are recommended for future work.

Possible applications are restricted, and examples for certain application are referred to.

A case reported in the literature of a railway sleeper was compared with the model estimate. The comparison highlighted the large errors to be expected both from the statistical data processing, which may be partially reduced, and from the definition of the relevant environmental data.

The preliminary development carried out allows having a better idea of the issues involved in modeling service life, and the lack of accuracy of course is not model dependent, but stresses the need of better data, procedures, models and understanding the basis of these

highly complex transformations. As in most things very complex processes only seldom can be modeled by relatively simple models.

To extend the application to higher expansions in actual concretes it would be convenient to adapt the model to alkali consumption (that in actual structures is no longer in excess as in the present tests with immersed bars), to the proportionality constant between extent of reaction and expansion, and to the aggregate size. These aspects may require additional tests not considered now.

Acknowledgments

The authors wish to acknowledge the Fundação para a Ciência e Tecnologia (FCT) for the financial support under project EXREACT (PTDC/CTM/65243/2006).

REFERENCES

[1] Swamy (Ed.), The Alkali–Silica Reaction in Concrete, Blackie, Glasgow and London, and Van Nostrand-Reinhold, New York, 1992.

[2] Larive, C., “Apports combinés de l'expérimentation et de la modélisation à la compréhension de l'alcali-réaction et de ses effets mécaniques”, Laboratoire Central des Ponts et Chaussées, (Rapport issu de thèse de doctorat de l'École Nationale des Ponts et Chaussées, soutenue le 6 juin 1997), Décembre 1998.

[3] Broekmans, M.A., “Guest Editorial”, Cement and Concrete Research, Vol. 40, 2010, p. 501.

[4] Scrivener, K.L., “Importance of microstructural understanding for durable and sustainable concrete”, Concrete Repair, Rehabilitation and Retrofitting II – Alexander et al (eds), Taylor and Francis Group, London, 2009.

[5] Poyet, S., “Etude de la dégradation des ouvrages en béton atteints par la réaction alcali-silice: Approche expérimentale et modélisation numérique multi-échelles des dégradations dans un environnement hydro-chemo-mécanique variable”, THÈSE grade de Docteur Génie Civil, l’Université de Marne-La-Vallée, Décembre 2003, Directeur de thèse Jean-Michel TORRENTI.

[6] Monnin, Y., “Méthodologie pour décrire le gonflement multi-échelle de calcaires siliceux soumis à la réaction alcali-silice dans le matériau béton”, These de Doctorat, Docteur de L’Universite d’Artois, Département Génie Civil de l’Ecole des Mines de Douai, Ecole Doctorale de l’Université d’Artois, Discipline: Génie Civil, Octobre 2005.

[7] Wigum, B.J., et al., “State-of-the art report: Key parameters influencing the alkali aggregate reaction”, Report 2.1, SINTEF, 2006.

[8] Wigum, B.J., “Alkali-Aggregate Reactions in Concrete Properties, Classification and Testing of Norwegian Cataclastic Rocks”, Dissertation submitted for the degree of Doktor Ingeniør, University of Trondheim, The Norwegian Institute of Technology, Department of Geology and Mineral Resources Engineering, December 1995.

[9] Goltermann, P., “Mechanical Predictions on Concrete Deterioration. Part 1: Eigenstresses in Concrete”, ACI Materials Journal, Vol. 91, No. 6, 1994, pp. 543-550.

[10] Goltermann, P., “Mechanical Predictions of Concrete Deterioration; Part 2: Classification of Crack Patterns”, ACI Materials Journal, Vol. 92, No.1, 1995, pp. 58-63.

[11] Pade, C., Struble, L., "Kinetics and Microstructural Changes Associated with Mortar Expansion", Cement, Concrete and Aggregates, Vol. 22, No. 1, 2000.

[12] Rivard, P., et al., "Alkali mass balance during the accelerated concrete prism test for alkali–aggregate reactivity", Cement and Concrete Research, Vol. 33, 2003, pp. 1147-1153.

[13] Moranville-Regourd, M., "Products of Reaction and Petrographic Examination", 8th International Conference on Alkali-Aggregate Reaction in Concrete, Kyoto, 1989, pp. 445-56.

[14] Katayama, T, Futagawa, T, "Diagenetic Changes in Potential Alkali-Aggregate Reactivity of Siliceous Sedimentary Rocks in Japan-A Geological Interpretation", 8th International Conference on Alkali-Aggregate Reaction, Kyoto, 1989, pp. 525-530.

[15] Furusawa, Y., Ohga, H., Uomoto, T., "An analytical study concerning prediction of concrete expansion due to alkali-silica reaction", In: Malhotra, Editor, 3rd Int. Conf. on Durability of Concrete, Nice, France, 1994, pp. 757–780 SP 145–40.

[16] ASTM C 289, "Standard Test Method for Potential Alkali-Silica Reactivity of Aggregates (Chemical Method)", ASTM International, West Conshohocken, United States, 2007.

[17] Shon , C.S., "Performance-Based Approach to Evaluate Alkali-Silica Reaction Potential of Aggregate and Concrete Using Dilatometer Method", Texas A&M University, May 2008.

[18] ASTM C 1260, "Standard test method for potential alkali reactivity of aggregates (mortar-bar method)", ASTM International, West Conshohocken, United States, 2007.

[19] Gonzalez, L.M., "Caracterização Cinética da Reacção Álcali-Sílica (RAS) no Betão, e Desenvolvimento de um Modelo para a sua Previsão", Relatório de Trabalho de Investigação Pós Doutoramento, Universidade do Minho, Maio 2010.

[20] Ben Haha, M., "Mechanical effects of alkali silica reaction in concrete studied by SEM-image analysis", Thèse No 3516, École Polytechnique Fédérale de Lausanne, Mai 2006.

[21] Helmuth, R., Stark, D., Diamond, S., Moranville-Regourd, M., "Alkali-Silica Reactivity: An Overview of Research", Monograph, SHRP-C-342 , Strategic Highway Research Program National Research Council, Washington DC, 1993.

[22] Capra B.; Bournazel J.P., "Modeling of Induced Mechanical Effects of Alkali-Aggregate Reactions", Cement and Concrete Research, Vol. 28, No. 2, 1998, pp. 251-260.

[23] Diamond, S., Barneyback, R.S., Struble, L.J., "On the physics and chemistry of alkali–silica reactions". In: Proceedings of the 5th International Conference on Alkali-Aggregate Reaction in Concrete, Cape Town, South Africa, 1981, S252/22.

[24] Bulteel, D., Garcia-Diaz, E., Siwak, J.M., Vernet, C., Zanni, H., "Alkali-aggregate reaction: A kinetic study", Congrès Infrastructure regeneration and rehabilitation improving the quality of life through better construction: a vision for the next millennium, Sheffield, 28 June - 2 July 1999, pp. 1041-1050.

[25] Gonzalez, L.M., Nogueira, C.A., Romero, J.B., "Comparação de modelos cinéticos para reacções heterogéneas não catalíticas, considerando tempo de indução" (Comparison of kinetic models for non catalytic heterogeneous reactions, considering induction time), 8th International Chemical Engineering Conf., (Ed. F. Ramôa Ribeiro e J.J. Cruz Pinto),

Aveiro, Setembro 2001, pp. 223-230.

[26] Johnston, D., Fournier, B.A., "A Kinetic-Based Method for Interpreting accelerated mortar bar test (ASTM C 1260) data", Proc. 11th International Conf. on Alkali-Aggregate Reaction, Quebec, 2000, pp. 355- 364.

[27] Moranville-Regourd, M., "Modelling of Expansion Induced by ASR–New Approaches", Cement and Concrete Composites, Vol. 19, 1997, pp. 415-425.

[28] Scrivener, K., Dunnant, C., "Modelling ASR with AMIE", Research progress conference, RILEM, Azores, 2010.

[29] Tsuneki, I., Masazumi, M., "Modified model of alkali-silica reaction", Cement and Concrete Research, Vol. 37, No. 9, September 2007, pp. 1291-1297.

[30] Glasser, L.S., Kataoka, N., "The chemistry of 'alkali-aggregate' reaction", Cement and Concrete Research, Vol. 11, No. 1, 1981, pp. 1-9.

[31] Scrivener, K.L., Monteiro, P.J.M., "The Alkali-Silica Reaction in a Monolithic Opal", Journal of the American Ceramic Society, Vol. 77, No. 11, 1994, pp. 2849-2856.

[32] Kawamura, M., Komatsu, S., "Behavior of Various Ions in Pore Solution in NaCl-bearing Mortar with and without Reactive Aggregate at Early Ages", Cement and Concrete Research, Vol. 27, No. 1, 1997, pp. 29-36.

[33] Miyagawa, T., Seto, K., Sasaki, K., Mikata, Y., Kuzume, K., and Minami, T., "Fracture of Reinforcing Steels in Concrete Structures Damaged by Alkali-Silica Reaction-Field Survey, Mechanism and Maintenance- ", Journal of Advanced Concrete Technology, Vol. 4, No. 3, 2006, pp. 339-355.

[34] Levenspiel, O., "Chemical Reaction Engineering", Wiley, 1972.

[35] Santos Silva, A., Gonçalves, A., Pipa, M., "Diagnosis and Prognosis of Portuguese Concrete Railway Sleepers Degradation – A Combination of ASR and DEF", ICAAR 2008, Trondheim, pp.164.